Phenomenology of mass-degenerate Higgs bosons in the NMSSM at the LHC

Biswaranjan Das*
IIT Guwahati

SUSY17
TIFR Mumbai

*(*B.D., S. Moretti, S. Munir, P. Poulose; Eur. Phys. J. C (2017) 77:544)*

Outline

- Introduction
- Diphoton production via gluon fusion: NWA and beyond
- Two Higgs bosons near 125 GeV
- Numerical setup
- Results
- Conclusions

Introduction

- NMSSM contains an extra Higgs singlet $\hat{S}$ in addition to the two MSSM Higgs doublets $\hat{H}_d$ and $\hat{H}_u$.
- 5 new parameters: λ, κ, A_λ, A_κ, v_s
- 5 neutral Higgs bosons; 3 scalars and 2 pseudoscalars in the real NMSSM (rNMSSM).
- Unlike the MSSM, CP violation can be invoked at the tree-level of the NMSSM Higgs sector,

$$\lambda = \mid \lambda \mid e^{i\phi_\lambda} \ , \ \kappa = \mid \kappa \mid e^{i\phi_\kappa}.$$

- 5 CP-mixed neutral Higgs states in the complex NMSSM (cNMSSM).

Diphoton production via gluon fusion: NWA and beyond

- The squared amplitude for $gg \to H_i \to \gamma\gamma$,

$$\mid \mathcal{M} \mid^2 = \sum_{\lambda,\sigma=\pm 1} \sum_{i=1,5} \mathcal{M}_{P_i\lambda} \mathcal{M}^*_{P_i\lambda} \left| D_{H_i}(\hat{s}) \right|^2 \mathcal{M}_{D_i\sigma} \mathcal{M}^*_{D_i\sigma} \,, \tag{1}$$

  λ, σ: gluon and photon helicities, $D_{H_i}(\hat{s})$: Higgs propagator matrix.

- Larger splitting between the Higgs boson masses $\implies$ NWA in the ith Higgs boson propagator

$$|D_i(\hat{s})|^2 = \left| \frac{1}{\hat{s} - m^2_{H_i} + i m_{H_i}\Gamma_{H_i}} \right|^2 \to \frac{\pi}{m_{H_i}\Gamma_{H_i}} \delta(\hat{s} - m^2_{H_i}). \tag{2}$$

- The partonic cross section

$$\hat{\sigma}(gg \to H_i \to \gamma\gamma) = \frac{1}{1024\pi\hat{s}} \sum_{i=1-5} \left(\sum_{\lambda=\pm} \left| \mathcal{M}_{P_i\lambda} \right|^2 \times \frac{\pi}{m_{H_i}\Gamma_{H_i}} \delta(\hat{s} - m^2_{H_i}) \times \sum_{\sigma=\pm} \left| \mathcal{M}_{D_i\sigma} \right|^2 \right). \tag{3}$$

- The cross section for the process $pp \to H_i \to \gamma\gamma$ in the NWA

$$\sigma(pp \to H_i \to \gamma\gamma) = \int_{\frac{m^2_{H_i}}{s}}^1 dx_1 \, \frac{1}{1024 s m^3_{H_i}\Gamma_{H_i}} \sum_{i=1-5} \left(\sum_{\lambda=\pm} \left| \mathcal{M}_{P_i\lambda} \right|^2 \sum_{\sigma=\pm} \left| \mathcal{M}_{D_i\sigma} \right|^2 \right) \frac{g(x_1) g(\frac{m^2_{H_i}}{s}/x_1)}{x_1}. \tag{4}$$

  $g(x)$ are the pdfs for the two gluons.

Diphoton production via gluon fusion: NWA and beyond

- Beyond the NWA: Two (or more) Higgs bosons are mass-degenerate near a given $\sqrt{\hat{s}} \implies$ need to consider the full propagator

$$D_H(\hat{s}) = \hat{s} \begin{pmatrix} \mathrm{m}_{11} + i\Im\mathrm{m}\hat{\Pi}_{11}(\hat{s}) & i\Im\mathrm{m}\hat{\Pi}_{12}(\hat{s}) & i\Im\mathrm{m}\hat{\Pi}_{13}(\hat{s}) & i\Im\mathrm{m}\hat{\Pi}_{14}(\hat{s}) & i\Im\mathrm{m}\hat{\Pi}_{15}(\hat{s}) \\ i\Im\mathrm{m}\hat{\Pi}_{21}(\hat{s}) & \mathrm{m}_{22} + i\Im\mathrm{m}\hat{\Pi}_{22}(\hat{s}) & i\Im\mathrm{m}\hat{\Pi}_{23}(\hat{s}) & i\Im\mathrm{m}\hat{\Pi}_{24}(\hat{s}) & i\Im\mathrm{m}\hat{\Pi}_{25}(\hat{s}) \\ i\Im\mathrm{m}\hat{\Pi}_{31}(\hat{s}) & i\Im\mathrm{m}\hat{\Pi}_{32}(\hat{s}) & \mathrm{m}_{33} + i\Im\mathrm{m}\hat{\Pi}_{33}(\hat{s}) & i\Im\mathrm{m}\hat{\Pi}_{34}(\hat{s}) & i\Im\mathrm{m}\hat{\Pi}_{35}(\hat{s}) \\ i\Im\mathrm{m}\hat{\Pi}_{41}(\hat{s}) & i\Im\mathrm{m}\hat{\Pi}_{42}(\hat{s}) & i\Im\mathrm{m}\hat{\Pi}_{43}(\hat{s}) & \mathrm{m}_{44} + i\Im\mathrm{m}\hat{\Pi}_{44}(\hat{s}) & i\Im\mathrm{m}\hat{\Pi}_{45}(\hat{s}) \\ i\Im\mathrm{m}\hat{\Pi}_{51}(\hat{s}) & i\Im\mathrm{m}\hat{\Pi}_{52}(\hat{s}) & i\Im\mathrm{m}\hat{\Pi}_{53}(\hat{s}) & i\Im\mathrm{m}\hat{\Pi}_{54}(\hat{s}) & \mathrm{m}_{55} + i\Im\mathrm{m}\hat{\Pi}_{55}(\hat{s}) \end{pmatrix}^{-1}, \tag{5}$$

with $\mathrm{m}_{ii} \equiv \hat{s} - m_{H_i}^2$, and $\Im\mathrm{m}\hat{\Pi}_{ij}(\hat{s})$: the absorptive parts of the Higgs self-energies, for $i, j = 1 - 5$.

- Full propagator matrix in the MSSM [J. Ellis et al., Phys.Rev. D70 (2004) 075010]. We generalized it in the NMSSM [B. Das et al., Eur. Phys. J. C (2017) 77:544].
- $\Im\mathrm{m}\hat{\Pi}_{ij}(\hat{s})$ become comparable to the Higgs mass difference. $i-$th Higgs state can undergo resonant transition to the $j-$th state, invalidating the NWA

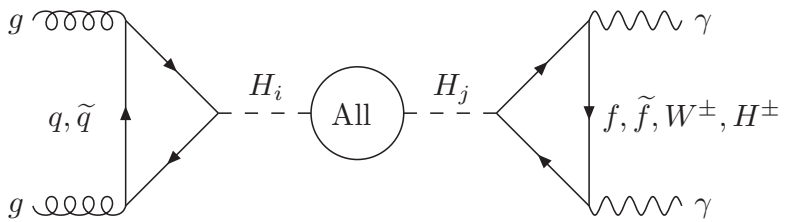

Diphoton production via gluon fusion: NWA and beyond

- The cross section beyond the NWA

$$\sigma(pp \to H_i \to H_j \to \gamma\gamma) = \int_0^1 d\tau \int_\tau^1 \frac{dx_1}{x_1} \frac{g(x_1)g(\tau/x_1)}{1024\pi\hat{s}^3} \sum_{i,j=1-5} \Big\{ \sum_{\lambda=\pm} \Big|\mathcal{M}_{P_i\lambda}\Big|^2 |D_{ij}(\hat{s})|^2 \sum_{\sigma=\pm} \Big|\mathcal{M}_{D_j\sigma}\Big|^2 \Big\}. \tag{6}$$

$g(x_1)$ and $g(\tau/x_1)$ are the pdfs of the two gluons.

- The differential cross section wrt τ

$$\frac{d\sigma}{d\tau} = \int_\tau^1 \frac{dx_1}{x_1} \frac{g(x_1)g(\tau/x_1)}{1024\pi\hat{s}^3} \sum_{i,j=1-5} \Big\{ \sum_{\lambda=\pm} \Big|\mathcal{M}_{P_i\lambda}\Big|^2 |D_{ij}(\hat{s})|^2 \sum_{\sigma=\pm} \Big|\mathcal{M}_{D_j\sigma}\Big|^2 \Big\}, \tag{7}$$

and then substituting $\tau = \frac{\hat{s}}{s} \implies d\tau = \frac{2\sqrt{\hat{s}}}{s} d\sqrt{\hat{s}}$ gives

$$\frac{d\sigma}{d\sqrt{\hat{s}}} = \int_\tau^1 \frac{2\sqrt{\hat{s}}}{s} \frac{dx_1}{x_1} \frac{g(x_1)g(\hat{s}/sx_1)}{1024\pi\hat{s}^3} \sum_{i,j=1-5} \Big\{ \sum_{\lambda=\pm} \Big|\mathcal{M}_{P_i\lambda}\Big|^2 |D_{ij}(\hat{s})|^2 \sum_{\sigma=\pm} \Big|\mathcal{M}_{D_j\sigma}\Big|^2 \Big\}. \tag{8}$$

Two Higgs bosons near 125 GeV

- CP-violating (CPV) scenarios where the observed Higgs resonance, can actually be explained by two mass-degenerate neutral Higgs states, give improved fit to the LHC data, compared to (a) the rNMSSM, (b) cNMSSM scenarios with a single Higgs boson $\sim$ 125 GeV. [S. Moretti et al., Adv. High Energy Phys. 2015, 509847 (2015)].

- Mass-degenerate scenarios with the full Higgs propagator have not been considered in the cNMSSM yet.

- **Objective:** To study the effect of the off-diagonal terms in the propagator matrix on the cross section of the process $pp \to H_i \to H_{obs} \to \gamma\gamma$, in the scenarios with two lightest Higgs bosons near 125 GeV in the rNMSSM as well as the cNMSSM.

Numerical setup

- **Model parameters:** Following universality conditions are used on the model parameters

$$M_0 \equiv M_{Q_{1,2,3}} = M_{U_{1,2,3}} = M_{D_{1,2,3}} = M_{L_{1,2,3}} = M_{E_{1,2,3}},$$
$$M_{\frac{1}{2}} \equiv 2M_1 = M_2 = \frac{1}{3}M_3, \qquad A_f \equiv A_{\tilde{t}} = A_{\tilde{b}} = A_{\tilde{\tau}}. \tag{9}$$

- **Mass-degeneracy condition:** $m_{H_2} - m_{H_1} < 2$ GeV (LHC mass resolution). [G. Aad et al. Phys. Rev. Lett. 114, 191803 (2015)]

- H_1 and H_2 are set to lie within 123-127 GeV to allow upto ± 2 GeV uncertainty coming from unknown higher order corrections in the model.

- **NMSSM Parameter set:** Three separate scans for the rNMSSM ($\phi_\kappa = 0^o$) and cNMSSM ($\phi_\kappa = 3^o$, 10^o). All other phases are set to 0^o.

NMSSM parameter	Scanned range
$M_0(\mathrm{GeV})$	800-2000
$M_{\frac{1}{2}}(\mathrm{GeV})$	100-500
$A_f(\mathrm{GeV})$	-3000-0
$\tan\beta$	2-8
λ	0.58-0.7
κ	0.3-0.6
$\mu_{eff}(\mathrm{GeV})$	100-200
$A_\lambda(\mathrm{GeV})$	200-1000
$A_\kappa(\mathrm{GeV})$	-300-0

Numerical setup

- The Higgs masses, couplings & branching ratios are extracted from the NMSSMCALC.
- The scanned points are passed to the HiggsBounds for consistency check of each Higgs with the LEP and LHC's direct search results. Also they are passed through various EDM constraints, computed by the NMSSMCALC.
- The 13 MeV upper limit on $\Gamma_{H_{obs}}$ at 95% CL in the combined ZZ^* and W^+W^- channels [CMS Col.,arXiv:1605.02329] is also imposed on each of Γ_{H_1,H_2}.
- We developed a fortran program to calculate the differential and the integrated cross sections, which is linked to LAPACK for propagator matrix inversion, and VEGAS for numerical integration.
- Our program calculates the leading order (LO) cross sections. For an approximate NNLO cross section, we multiplied the LO cross section by $k_{\rm NNLO} = 3$ (calculated by the SusHi).

Results

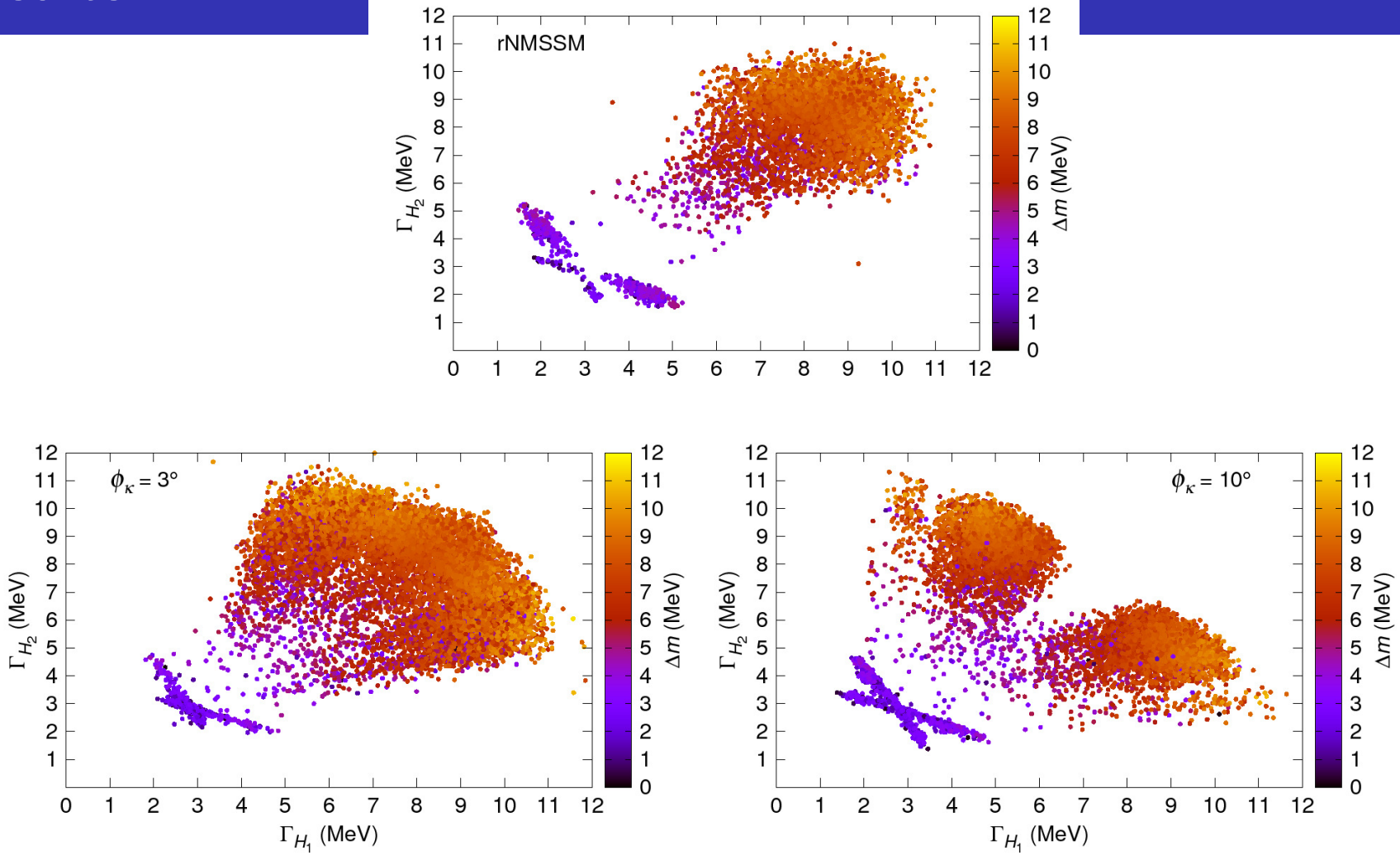

Figure: : Points obtained from the parameter space scans of the rNMSSM (top) and of the cNMSSM with $\phi_\kappa = 3°$ (bottom left) and with $\phi_\kappa = 10°$ (bottom right). For all the points shown, $\Delta m = m_{H_2} - m_{H_1}$ (colour map) is always smaller than Γ_{H_1} (x-axis) and/or Γ_{H_2} (y-axis).

Results

- We studied the differential cross section distributions w.r.t. $\sqrt{\hat{s}}$ for $pp \to H_i \to H_{obs} \to \gamma\gamma$ for the following three cases:

  case 1: Two independent Breit-Wigners (BWs).

  case 2: With tree-level interference between H_1 and H_2 but without any mixing effects.

  case 3: Non-zero off-diagonal terms in the proagator matrix, leading to additional interference effects due to the mixing of H_1 and H_2.

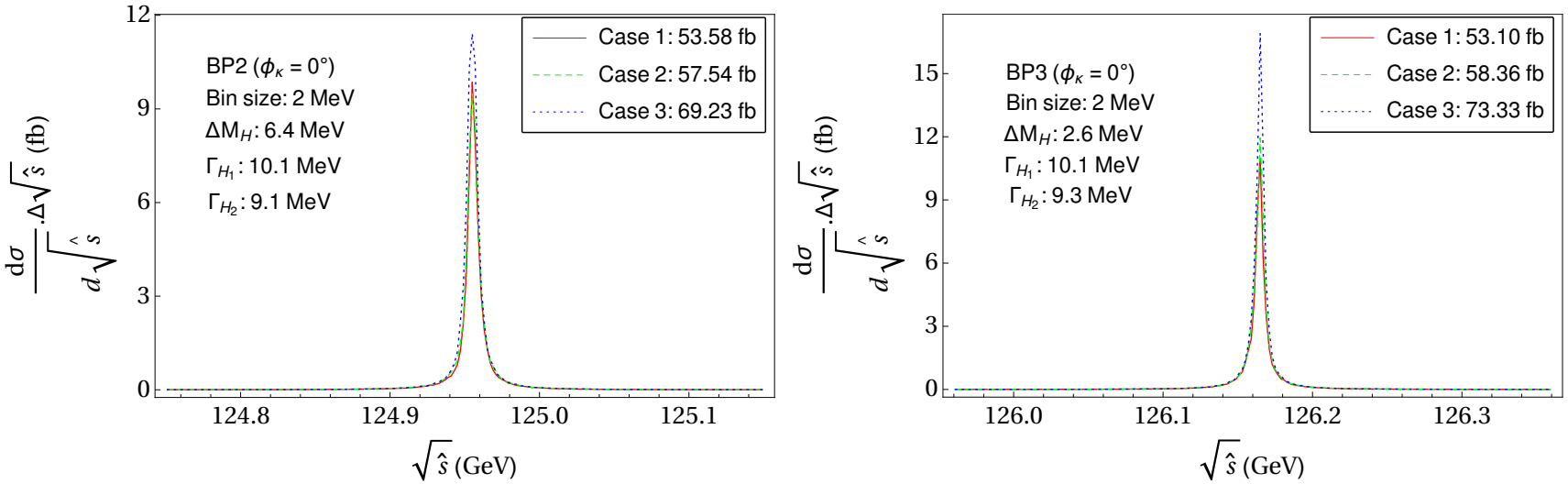

Figure: Distributions for two selected BPs in the rNMSSM. The red, green and blue curves correspond to the case 1, 2 and 3, respectively.

Results

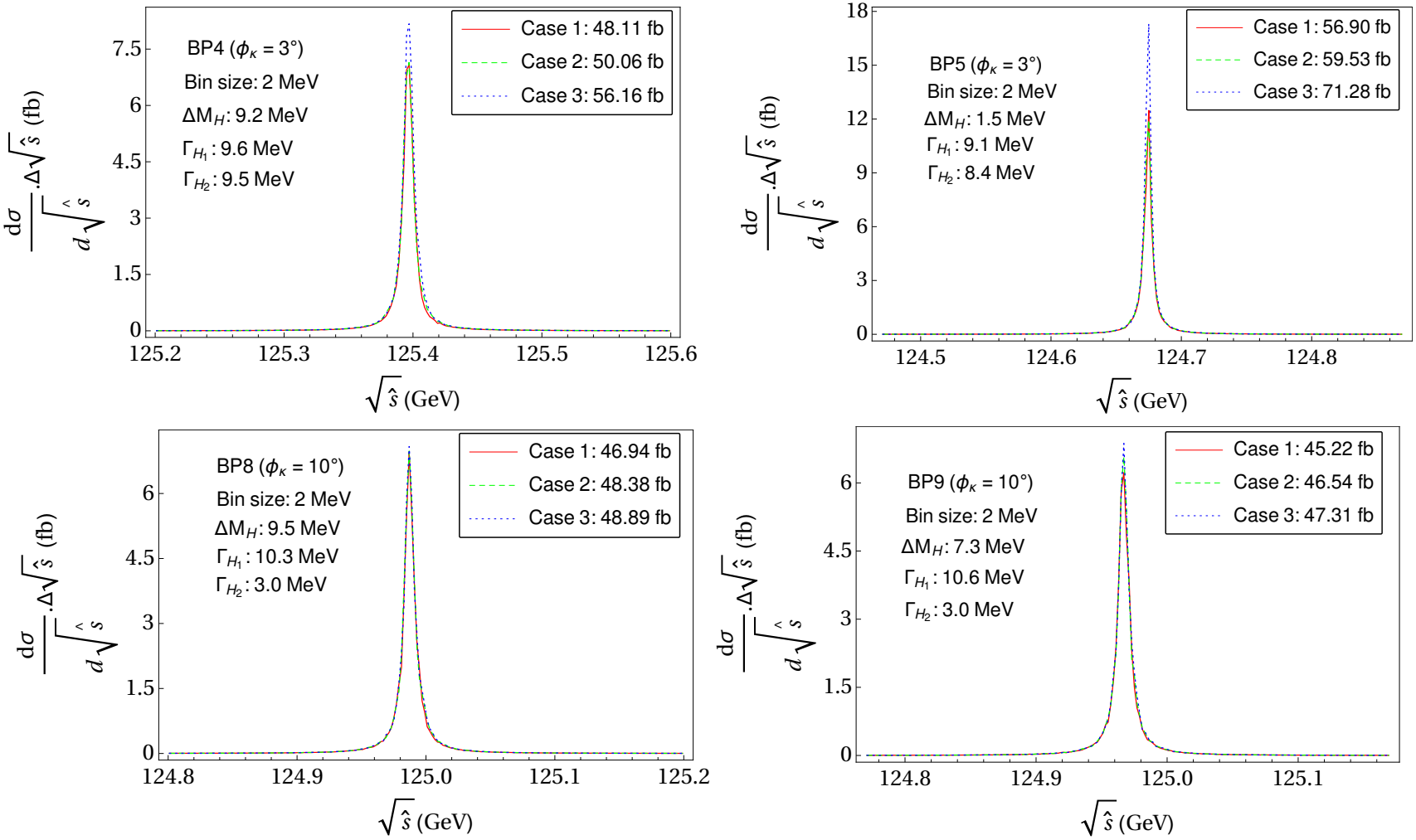

Figure: Distributions for the BPs in the cNMSSM with $\phi_\kappa = 3°$ (top panel) and $\phi_\kappa = 10°$ (bottom panel).

Results

- We considered the possibility of shape analysis between case 1 and case 3, which could reveal the presence of multiple resonances, assuming realistic, current and prospective, detector facilities.

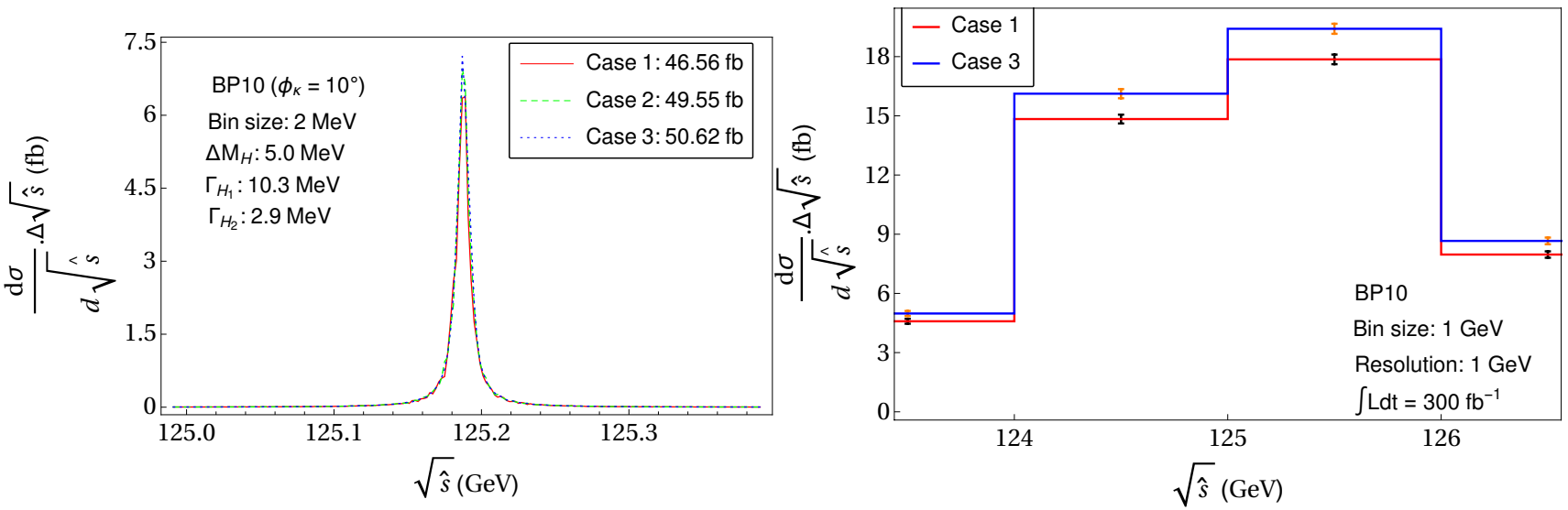

Figure: Distributions for a selected BP before convolution (left) and after convolution with a Gaussian of width 1 GeV for an integrated luminosity 300 fb^{-1} (right).

Results

- The difficulty to separate Case 1 and 3 for BP10 at the LHC is due to the the $\Gamma_{H_1,H_2} < 13 MeV$ constraint. This could be ignored, since the current procedures for extracting the Higgs boson properties, assumed that only one resonance could appear near 125 GeV.
- Hence we selected few test points (TPs), relaxing the decay width constraint.

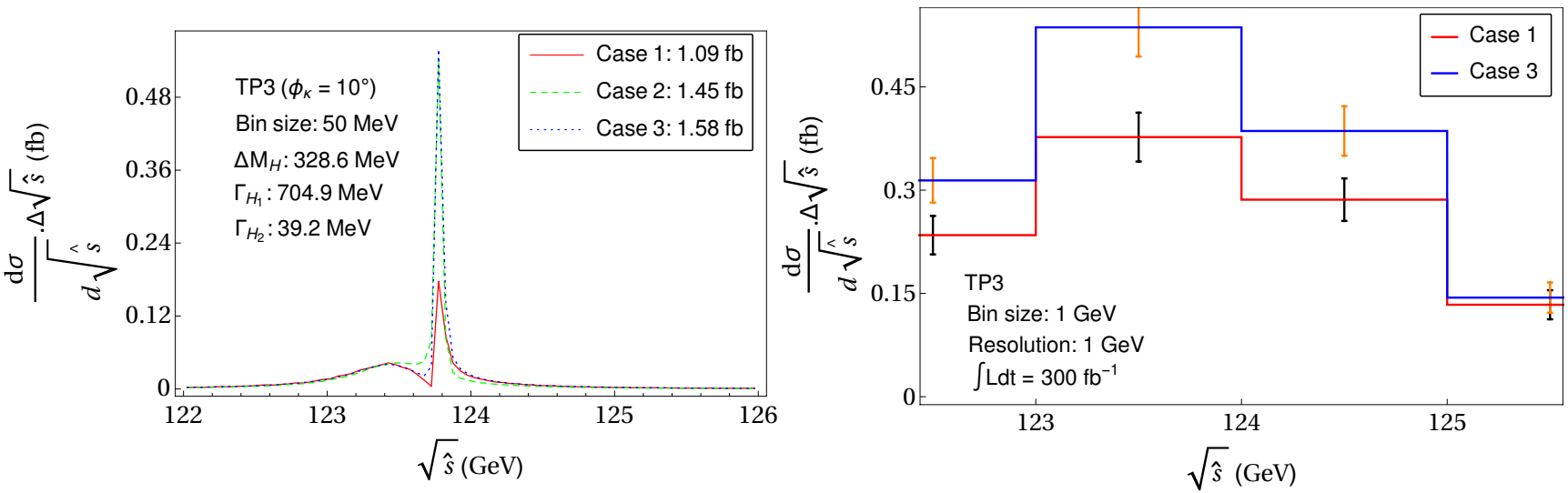

Figure: Distributions for a selected TP before (left) and after convolution (righ).

Conclusions

- Our analysis do not exclude the possibility of non-SM explanations, particularly those with two Higgs bosons with such a small mass difference that they cannot be resolved at the current experimental facilities.
- This particular possibility can emerge only in non-minimal realisations of SUSY, such as the NMSSM.
- Interference effects could be sizable, up to around 40% in cross sections, between the standard approach of treating the two resonances separately and the full propagator.
- We also considered the possibility of shape analysis of the emerging profiles, which revealed some long-term potential to observe experimentally the difference between case 1 and case 3.

Thank You